Time-resolved UV-visible spectroelectrochemistry using transparent 3D-mesoporous nanocrystalline ITO electrodes†

Christophe Renault,[a] Kenneth D. Harris,[b] Michael J. Brett,[bc] Véronique Balland*[a] and Benoît Limoges*[a]

Received 30th September 2010, Accepted 15th November 2010
DOI: 10.1039/c0cc04154h

Efficient and rapid adsorption of microperoxidase 11 within a highly porous ITO thin film (200 nm) prepared by glancing angle deposition was achieved. Adsorbed redox molecules were reversibly and rapidly reduced throughout the 3D-conductive matrix in *ca.* 50 ms, allowing the heterogeneous electron transfer rate to be determined by derivative cyclic voltabsorptometry.

Because of their high surface area and unique electrical and optical properties, transparent nanostructured metal oxide films offer new opportunities to design biosensors as well as to develop spectroelectrochemical methods for investigating redox biomolecules immobilized within these matrices.[1–3] The latter has been well-illustrated by the study of direct electron transfer between nanocrystalline SnO_2 electrodes and redox proteins absorbed on the metal oxide surface.[4–7] In particular it was found that cross-correlations between electrochemical and optical data can be very useful in elucidating some thermodynamic and kinetic aspects of these systems. However, major drawbacks with these semiconductive nanoporous SnO_2 films are poor pore accessibility[6] and acceptable conductivities limited to potentials < 0.2 V (*vs.* ECS).[7] For more positive potentials, the electrode Fermi level lies within the semiconductor bandgap, and the film is therefore insulating. In order to overcome this limitation, we propose here to use mesoporous conductive films of tin-doped indium oxide (ITO), which with metal-like properties can accommodate a much wider potential window, restricted only by the solvent discharge. Another expected advantage is increased electronic conduction that should lead to faster electron transport than in semiconductor films and pave the way for developing a time-resolved spectroelectrochemistry of adsorbed redox proteins.

For such a purpose, the porous ITO film must satisfy the following specifications: (i) a well-accessible mesoporosity to achieve rapid incorporation of relatively large biomolecules, (ii) a high specific surface area to adsorb the maximum quantity of biomolecules and achieve a measurable optical density and (iii) a high electrical conductivity to rapidly convert adsorbed redox biomolecules electrochemically. The last two are important insofar as they may determine the time resolution of the method, which can be limited either by insufficient signal-to-noise ratio in spectroscopy or by slow electron transport kinetics within the mesoporous material.

The preparation of thin conductive films of doped metal oxide with a controlled porosity and transparency has been achieved only recently by two different strategies.[8–11] One is based on an hybrid organic–inorganic sol–gel process which allows thin films of doped metal oxide to be produced with a 3D-mesoporosity.[8,9] The main advantage of this method is the ability to generate well-ordered nanoporous structures, but restricted film thicknesses as well as porosity (maximal pore size of ~15–20 nm) have been observed. Mesoporous ITO films obtained with this method were recently proposed for the adsorption and spectroelectrochemical characterization of cytochrome c.[12] A second approach is vacuum-based glancing angle deposition (GLAD), a single-step physical vapor-deposition technique that leads to the formation of highly porous films made of nanosized columnar structures.[10,11] The main advantage of this technique is that it allows the production of mesoporous nanocrystalline films of ITO with easily adjustable thickness, porosity, surface area, and shape.[11]

In the present work, we report the immobilization of microperoxidase 11 (MP-11) within 200 nm thick nanocrystalline GLAD ITO films grown on ITO coated glass slides, using an oblique deposition angle of 75° (Fig. 1).[11] MP-11 was selected as an ideal one-electron redox protein because it (i) exhibits a very intense absorption band around 400 nm (Soret band) characteristic of the heme redox state (*i.e.*, Fe^{III}/Fe^{II} couple), and (ii) has a small size to allow direct electron transfer and high surface coverage to be achieved. MP-11 was adsorbed within the thin film by soaking the electrode in 50 μM MP-11, and after equilibration, the resulting electrode was investigated by UV-visible spectroscopy in a protein-free HEPES buffer. A clear and well-defined Soret band of adsorbed MP-11 was observed at $\lambda = 405$ nm (Fig. S1, ESI†), most likely indicative of a low-spin hexacoordinated heme.[13] From the plot of the

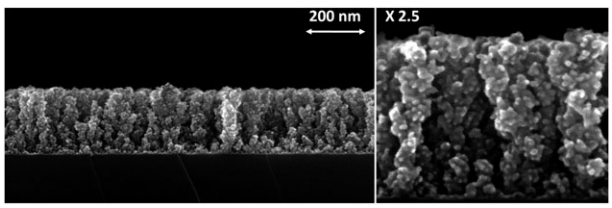

Fig. 1 Scanning electron micrograph of an ITO GLAD vertical post film at $\alpha = 75°$, showing nanopost diameters of ~50 nm and pores of ~30 nm.

[a] *Laboratoire d'Electrochimie Moléculaire, Université Paris Diderot, UMR CNRS 7591, 15, rue Jean-Antoine de Baïf, 75205 Paris Cedex 13, France. E-mail: veronique.balland@univ-paris-diderot.fr, limoges@univ-paris-diderot.fr; Tel: +33 157278789*
[b] *National Research Council (NRC), National Institute for Nanotechnology (NINT), Edmonton, Alberta, Canada T6G 2M9*
[c] *Electrical and Computer Engineering, University of Alberta, Edmonton, Alberta, Canada T6G 2V4*

† Electronic supplementary information (ESI) available: Experimental and instrumental details. Fig. S1–S5. See DOI: 10.1039/c0cc04154h

Soret band absorbance as a function of soaking time, a first-order adsorption rate constant of $k_{ads} = 0.18$ min^{-1} was determined, indicating that saturation of the electrode was almost reached after 20 min of immersion. Desorption of a saturated electrode in a protein-free buffer shows that ~20% of adsorbed MP-11 is rapidly desorbed, whereas the remaining 80% is quite stable over a few hours. Assuming that the extinction coefficient of the adsorbed peptide is $\varepsilon_{405} \approx 10^5$ M^{-1} cm^{-1}, the surface concentration of MP-11 can be estimated, and a value of $\Gamma \approx 10^{-9}$ mol cm^{-2} was obtained for the film free of poorly adsorbed MP-11. This value is equivalent to 38-fold that which can be predicted geometrically for a close-packed monolayer on a perfectly flat surface (*i.e.* $\Gamma = 2.6 \times 10^{-11}$ mol cm^{-2}, taking the size of each MP-11 molecule along the projection of terminal amine to be 6.2 nm^2).[14] This result is consistent with the specific surface area enhancement of 200-fold per μm of film thickness (*i.e.*, equivalent to an enhancement of 40 for the 200 nm films used) that was previously determined for ITO films deposited at an angle of 75°.[11]

Spectroelectrochemical titration of the strongly adsorbed MP-11 was realized in a home-made spectroelectrochemical cell that was thoroughly bubbled with argon for 30 min prior to experiments. Reduction of MP-11 was observed to be fully reversible, with well-defined isosbestic points at 410, 447 and 509 nm (Fig. S2, ESI†) in the difference spectra. The resulting titration curve was adjusted to the Nernst equation, and in the best fit, a standard potential of $E^{0\prime} = -0.35$ V *vs.* Ag/AgCl was obtained for $n = 0.4$ electrons transferred. This value of n is far from the value of 1 expected for the one-electron Fe^{III}/Fe^{II} couple. This low value for n can be attributed to the distribution of MP-11 in various microenvironments and/or orientations on the surface, as previously reported for microperoxidase and other hemoproteins.[15,16] The Nernst curve was therefore fitted assuming a square distribution of standard potentials and $n = 1$.[16] The best fit gave an average standard potential value $E^{0\prime,av}$ of −0.35 V and a ΔE of 0.15 V (Fig. S2, ESI†). The $E^{0\prime,av}$ is close to that reported for the molecule in homogeneous solution ($E^{0\prime} = -0.38$ V).

In addition to the thermodynamic analysis, the time-dependence of the redox changes (Fe^{III}/Fe^{II}) following a series of normal pulse potential steps was monitored at 420 nm. The resulting chronoabsorptometric trace is shown in Fig. 2 for the reductive scan (see Fig. S3, ESI† for the oxidative scan). An integration time of 20 ms was selected for the diode array detector to allow a sufficient absorbance signal-to-noise ratio, and an ohmic drop compensation was applied during the cyclic scan to minimize the time constant of the electrochemical cell. The reduction–reoxidation cycle of adsorbed MP-11 could be performed hundreds of time without significant loss of absorbance, indicating that the two redox states are stable under redox cycling and that the MP-11 is firmly anchored on the ITO surface, whatever its redox state. Although difficult to discern in Fig. 2, it appears that the rate of reduction is accelerated as the applied cathodic potential is increased and reaches a maximum rate at a negative potential of −0.6 V (*i.e.*, at a favorable driving force of ~250 mV). Below this potential, the adsorbed MP-11 is fully reduced according to a single exponential decay with a time constant of

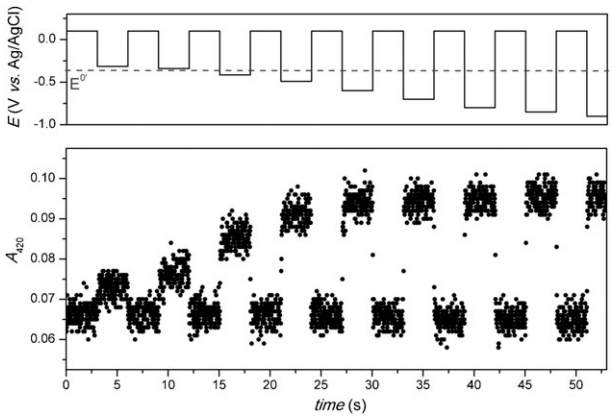

Fig. 2 Absorbance (●) of a mesoporous ITO electrode loaded with MP-11 ($\Gamma_{MP\text{-}11} = 8 \times 10^{-10}$ mol cm^{-2}) and monitored at $\lambda = 420$ nm during a series of normal pulse potential steps (black line) from 0.1 to −0.315, −0.34, −0.415, −0.49, −0.6, −0.7, −0.8, −0.85 and −0.9 V *vs.* Ag/AgCl. Integration time: 20 ms; 0.1 M HEPES, pH 7.0.

30 ms (Fig. S4, ESI†), independent of the applied overpotential. The same rate limit was obtained for the reoxidation of MP-11. We attribute this limit to the time constant, $R_{cell}C_{dl}$, of the electrochemical cell (where R_{cell} is the cell resistance and C_{dl} the cell double layer capacitance). Considering that after ohmic drop correction, R_{cell} remains a few ohms and that the C_{dl} value extracted from cyclic voltammograms is ~400 μF, a cell time constant of about 10 ms can be estimated, which is close to 30 ms found by chronoabsorptometry. From the maximal variation of absorbance measured in the difference spectra at 420 nm, a surface concentration of $\Gamma = (8 \pm 1) \times 10^{-10}$ mol cm^{-2} of electroactive MP-11 can be determined using $\Delta\varepsilon_{420} = \varepsilon_{red} - \varepsilon_{ox} = 42\,000$ M^{-1} cm^{-1}.[17] This value is in fairly good agreement with the total quantity of native MP-11 that was initially adsorbed into the film (*i.e.*, 10^{-9} mol cm^{-2}), indicating that nearly all of the adsorbed MP-11 molecules are in direct electrical communication with the conductive mesostructure of ITO.

In an attempt to learn more regarding electron transport through the film, ITO electrodes loaded with MP-11 were simultaneously scanned by cyclic voltammetry and UV-visible spectroscopy. The resulting variation of absorbance as a function of time, and therefore potential, was used to plot cyclic voltabsorptograms (CVAs) and their respective derivatives (DCVAs), which have greater selectivity and freedom from capacitive current than cyclic voltammograms (Fig. S5, ESI†).[18] Two illustrating examples of CVAs and DCVAs obtained at two scan rates (v) are given in Fig. 3. At low scan rates, a well-defined symmetrical pair of redox peaks, characteristic of the Fe^{III}/Fe^{II} couple, is observed at $E^{0\prime} = -0.35$ V. An analysis of the cathodic and anodic peak intensities in DCVAs as a function of v shows a linear dependence up to a scan rate of 1 V s^{-1} (Fig. 3C), whereas the magnitude of absorbance changes in CVAs remains constant up to 5 V s^{-1} (Fig. 3A). All of these are characteristics of a thin-layer redox process, where all molecules contained within the film are rapidly converted to their oxidized or reduced form in the time scale of the experiment. The kinetics of electron transfer were investigated by measuring the peak

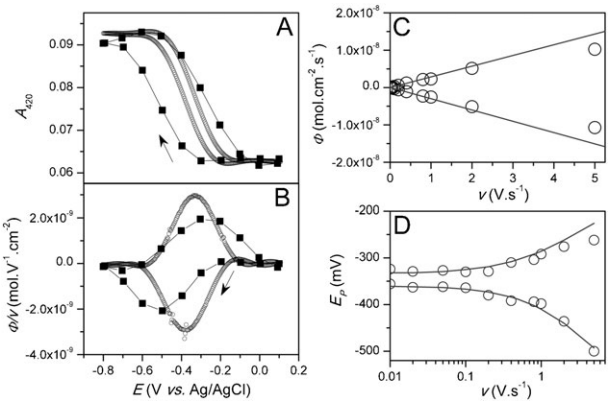

Fig. 3 (A) CVAs and (B) DCVAs (expressed as flux density normalized to v) of a mesoporous ITO electrode saturated with MP-11, recorded at 420 nm and at (○) 0.2 and (■) 5 V s^{-1}. Integration time: 20 ms; 0.1 M HEPES, pH 7.0. The arrow indicates scan direction. Plots of (C) flux density and (D) peak potential of DCVA as a function v. Lines: (C) linear fitting to the flux density and (D) nonlinear fit obtained from simulation of the Butler–Volmer equations and using $\alpha = 0.4$ and $k^0 = 10$ s^{-1}.

potential difference (ΔE_P) between the anodic and cathodic waves of DCVAs as a function of the scan rate (Fig. 3D). Upon raising the scan rate, the increase of ΔE_P at $v > 1$ V s^{-1} reflects the progressive kinetic control limited by the rate of heterogeneous electron transfer from immobilized MP-11. The data were thus fitted to the theoretical peak potential values calculated from classical Butler–Volmer equations under thin-layer conditions. From the best fit, a heterogeneous electron transfer rate constant of $k^0 = 10$ s^{-1} and charge transfer coefficient of $\alpha = 0.4$ were obtained.

The highest scan rate used in cyclic voltabsorptometry, *i.e.* 5 V s^{-1}, is close to the time resolution of the method, which is limited by the 30 ms cell time constant. Given this time limit, one question that arises concerns the mode of electron transport within the film. For a redox species immobilized within a semiconductive or conductive film, there are three different electron transport mechanisms: (i) by physical diffusion to the underlying plain ITO electrode, (ii) by electron hopping between redox centers, and (iii) by electron transport through the conducting 3D-matrix. The characteristic time constant of 30 ms indicates the upper limit of electron transport that is accessible under our conditions. It is equivalent to the time required for a molecule having an apparent diffusion coefficient of 10^{-8} cm^2 s^{-1} to diffuse throughout the 200 nm thick film. On account of the strong binding of MP-11 to ITO, such a value is too fast to be dominated by simple electron transport by physical diffusion, which normally should be more than 1000-fold slower.[19] It is also unlikely that it should result from fast electron hopping between adsorbed MP-11 because we have observed no change in the time constant after varying the concentration of MP-11 within the film (Fig. S4, ESI†). Therefore, the unique way to reasonably explain the fast rate of absorbance changes is through a rapid electron transport throughout the conductive 3D-structure of ITO, a process that is unfortunately currently masked by the cell time constant.

In summary, we have demonstrated that mesoporous nanocrystalline ITO thin films obtained by the glancing angle deposition technique can be advantageously used as 3D-transparent electrodes for time-resolved UV-visible spectroelectrochemistry of an adsorbed redox protein. The accessible time resolution for kinetics studies is currently on the order of a few tens of milliseconds, mainly limited by the electrochemical cell time constant. Under these conditions, we were able to determine a heterogeneous electron transfer rate constant of 10 s^{-1}. The methodology should thus provide a powerful approach to monitor reaction kinetics of adsorbed proteins or enzymes up to a temporal resolution of *ca.* 50 ms. It is also noteworthy that the temporal resolution might be improved significantly by reducing the cell time constant, $R_{cell}C_{dl}$; an outcome that could be easily achieved by decreasing the electrode size and, consequently, the electrode capacitance, or by altering the ionic strength, nature of the electrolyte counter ions, and/or buffer composition in such a way to reduce both R_{cell} and C_{dl}. Work aimed at achieving this goal is currently in progress.

Support for this work was provided by Micralyne, NSERC, and Alberta Innovates: Technology Futures.

Notes and references

1 E. Topoglidis, C. J. Campbell, A. E. G. Cass and J. R. Durrant, *Electroanalysis*, 2006, **18**, 882–887.
2 X. Xu, B. Tian, J. Kong, S. Zhang, B. Liu and D. Zhao, *Adv. Mater.*, 2003, **15**, 1932–1936.
3 G. L. Kemp, S. J. Marritt, L. I. Xiaoe, J. R. Durrant, M. R. Cheesman and J. N. Butt, *Biochem. Soc. Trans.*, 2009, **37**, 368–372.
4 Y. Astuti, E. Topoglidis, P. B. Briscoe, A. Fantuzzi, G. Gilardi and J. R. Durrant, *J. Am. Chem. Soc.*, 2004, **126**, 8001–8009.
5 S. J. Marritt, G. L. Kemp, L. Xiaoe, J. R. Durrant, M. R. Cheesman and J. N. Butt, *J. Am. Chem. Soc.*, 2008, **130**, 8588–8589.
6 P. Panicco, Y. Astuti, A. Fantuzzi, J. R. Durrant and G. Gilardi, *J. Phys. Chem. B*, 2008, **112**, 14063–14068.
7 E. Topoglidis, Y. Astuti, F. Duriaux, M. Grätzel and J. R. Durrant, *Langmuir*, 2003, **19**, 6894–6900.
8 D. Fattakhova-Rohlfing, T. Brezesinski, J. Rathouský, A. Feldhoff, T. Oekermann, M. Wark and B. M. Smarsly, *Adv. Mater.*, 2006, **18**, 2980–2983.
9 Y. Wang, T. Brezesinski, M. Antonietti and B. Smarsly, *ACS Nano*, 2009, **3**, 1373–1378.
10 K. Robbie, J. C. Sit and M. J. Brett, *J. Vac. Sci. Technol., B*, 1998, **16**, 1115–1122.
11 K. M. Krause, M. T. Taschuk, K. D. Harris, D. A. Rider, N. G. Wakefield, J. C. Sit, J. M. Buriak, M. Thommes and M. J. Brett, *Langmuir*, 2010, **26**, 4368–4376.
12 S. Frasca, T. von Graberg, J.-J. Feng, A. Thomas, B. M. Smarsly, I. M. Weidinger, F. W. Scheller, P. Hildebrandt and U. Wollenberger, *ChemCatChem*, 2010, **2**, 839–845.
13 P. A. Adams, D. A. Baldwin and H. M. Marques, in *Cytochrome c: a Multidisciplinary Approach*, ed. R. A. Scott and A. G. Mauk, University Science Books, Sausalito, California, 1996, pp. 635–692.
14 L. Jiang, A. Glidle, C. J. McNeil and J. M. Cooper, *Biosens. Bioelectron.*, 1997, **12**, 1143–1155.
15 D. H. Murgida and P. Hildebrandt, *J. Mol. Struct.*, 2001, **565–566**, 97–100.
16 V. Balland, S. Lecomte and B. Limoges, *Langmuir*, 2009, **25**, 6532–6542.
17 Assuming that $\Delta\varepsilon_{420}$ is the same as that of a homogeneous solution of 15 μM MP-11 in phosphate buffer, pH 7.0.
18 E. E. Bancroft, J. S. Sidwell and H. N. Blount, *Anal. Chem.*, 1981, **53**, 1390–1394.
19 S. A. Trammell and T. J. Meyer, *J. Phys. Chem. B*, 1999, **103**, 104–107.